2008 American Control Conference
Westin Seattle Hotel, Seattle, Washington, USA
June 11-13, 2008

Asymptotic Tracking for Aircraft via an Uncertain Dynamic Inversion Method

W. MacKunis[†], M. K. Kaiser[‡], P. M. Patre[†], and W. E. Dixon[†]
[†]Mechanical and Aerospace Engineering Department, University of Florida, Gainesville, FL 32611-6250
[‡]Air Force Research Laboratory, Munitions Directorate, Eglin AFB, FL 32542-6810
Email: mackunis@ufl.edu, michael.kaiser@eglin.af.mil, pmpatre@ufl.edu, wdixon@ufl.edu

Abstract— **An asymptotic tracking controller is designed in this paper, which combines Model Reference Adaptive Control (MRAC) and Dynamic Inversion (DI) methodologies in conjuction with the robust integral of the signum of the error (RISE) technique for output tracking of an aircraft system in the presence of parametric uncertainty and unknown, nonlinear disturbances, which are not linearly parameterizable (non-LP). The control design is complicated by the fact that the control input is multiplied by an uncertain, non-square matrix. Partial knowledge of the aircraft model along with constant feedforward estimates of the unknown plant parameters are exploited in order to reduce the required control effort. This result shows for the first time how asymptotic tracking control can be achieved for a nonlinear system in the presence of a non-square input matrix containing parametric uncertainty and nonlinear, non-LP disturbances. Asymptotic output tracking is proven via Lyapunov stability analysis, and high-fidelity simulation results are provided to verify the efficacy of the proposed controller.**

I. Introduction[1]

Feedback linearization is a general control method where the nonlinear dynamics of a system are canceled by state feedback yielding a residual linear system. Dynamic inversion is a similar concept as feedback linearization that is commonly used within the aerospace community to replace linear aircraft dynamics with a reference model [1]–[9]. For example, a general dynamic inversion approach is presented in [4] for a reference tracking problem for a minimum-phase and left-invertible linear system. A dynamic inversion controller is designed for a nonminimum-phase hypersonic aircraft system in [2], which utilizes an additional controller to stabilize the zero dynamics. A finite-time stabilization design is proposed in [3], which utilizes dynamic inversion given a full rank input matrix. Typically, dynamic inversion methods (e.g., [1], [2]) assume the corresponding plant models are exactly known. However, parametric uncertainty, additive disturbances, and unmodeled plant dynamics are always present in practical systems.

Motivated by the desire to improve the robustness to uncertainty over traditional methods, adaptive dynamic inversion (ADI) was developed as a method to compensate for parametric uncertainty (cf. [4], [6], [7], [9]). Typically, ADI methods exploit model reference adaptive control (MRAC) techniques where the desired input-output behavior of the closed-loop system is given via the corresponding dynamics of a reference model [5], [7], [10]. Therefore, the basic task is to design a controller which will ensure the minimal error between the reference model and the plant outputs despite uncertainties in the plant parameters and working conditions. Several efforts (e.g., [8], [9], [11]–[14]) have been developed for the more general problem where the uncertain parameters or the inversion mismatch terms do not satisfy the linear-in-the-parameters assumption (i.e., non-LP). One method to compensate for non-LP uncertainty is to exploit a neural network as an on-line function approximation method as in [11]–[13]; however, all of these results yield uniformly ultimately bounded stability due to the inherent function reconstruction error.

In contrast to neural network-based methods to compensate for the non-LP uncertainty, a robust control approach was recently developed in [15] (coined RISE control in [16]) to yield an asymptotic stability result. The RISE-based control structure has been used for a variety of fully actuated systems in [15]–[18]. The contribution in this result is the use of the RISE control structure to achieve asymptotic output tracking control of a model reference system, where the plant dynamics contain a bounded additive disturbance (e.g., potential disturbances include: gravity, inertial coupling, nonlinear gust modeling, etc.). This result represents the first ever application of the RISE method where the controller is multiplied by a non-square matrix containing parametric uncertainty. To achieve the result, the typical RISE control structure and closed-loop error system development are modified by adding a robust control term, which is designed to compensate for the uncertainty in the input matrix. The result is proven via Lyapunov-based stability analysis and demonstrated through numerical simulation.

II. Aircraft Model and Properties

The aircraft system under consideration in this paper can be modeled via the following state space representation [2], [6]:

[1]This research is supported in part by the NSF CAREER AWARD 0547448, NSF SGER 0738091, AFOSR contract numbers F49620-03-1-0381 and F49620-03-1-0170, AFRL contract number FA4819-05-D-0011, Department of Energy URPR program grant number DE-FG04-86NE37967, and by research grant No. US-3715-05 from BARD, the United States - Israel Binational Agricultural Research and Development Fund.

$$\dot{x} = Ax + Bu + f(x,t) \quad (1)$$
$$y = Cx, \quad (2)$$

where $A \in \mathbb{R}^{n\times n}$ denotes the state matrix, $B \in \mathbb{R}^{n\times m}$ for $m < n$ represents the input matrix, $C \in \mathbb{R}^{m\times n}$ is the known output matrix, $u \in \mathbb{R}^m$ is a vector of control inputs, and $f(x,t) \in \mathbb{R}^n$ represents an unknown, nonlinear disturbance.

Assumption 1: The A and B matrices given in (1) contain parametric uncertainty.

Assumption 2: The nonlinear disturbance $f(x,t)$ and its first two time derivatives are assumed to exist and be bounded by a known constant.

A. Osprey Aircraft Model

In this section, we describe how a specific aircraft can be related to (1). The Osprey fixed wing aerial vehicle (see Fig. 1) is a commercially available, low-cost experimental flight test bed for investigating novel control approaches. Based

Fig. 1. The Osprey aircraft testbed.

on the standard assumption that the longitudinal and lateral modes of the aircraft are decoupled, the state space model for the Osprey aircraft testbed can be represented using (1) and (2), where the state matrix $A \in \mathbb{R}^{8\times 8}$ and input matrix $B \in \mathbb{R}^{8\times 4}$ are given as

$$A = \begin{bmatrix} A_{lon} & 0_{4\times 4} \\ 0_{4\times 4} & A_{lat} \end{bmatrix} \qquad B = \begin{bmatrix} B_{lon} & 0_{4\times 2} \\ 0_{4\times 2} & B_{lat} \end{bmatrix}, \quad (3)$$

and the output matrix $C \in \mathbb{R}^{4\times 8}$ is designed as

$$C = \begin{bmatrix} C_{lon} & 0_{2\times 4} \\ 0_{2\times 4} & C_{lat} \end{bmatrix}, \quad (4)$$

where $A_{lon}, A_{lat} \in \mathbb{R}^{4\times 4}$, $B_{lon}, B_{lat} \in \mathbb{R}^{4\times 2}$, and $C_{lon}, C_{lat} \in \mathbb{R}^{2\times 4}$ denote the state matrices, input matrices, and output matrices, respectively, for the longitudinal and lateral subsystems, and the notation $0_{i\times j}$ denotes an $i \times j$ matrix of zeros. The state vector $x(t) \in \mathbb{R}^8$ is given as

$$x = \begin{bmatrix} x_{lon}^T & x_{lat}^T \end{bmatrix}^T, \quad (5)$$

where $x_{lon}(t), x_{lat}(t) \in \mathbb{R}^4$ denote the longitudinal and lateral state vectors defined as

$$x_{lon} \triangleq \begin{bmatrix} V & \alpha & q & \theta \end{bmatrix}^T \qquad x_{lat} \triangleq \begin{bmatrix} \beta & p & r & \phi \end{bmatrix}^T, \quad (6)$$

where the state variables are defined as

$$V = velocity \qquad \alpha = angle\ of\ attack$$
$$q = pitch\ rate \qquad \theta = pitch\ angle$$
$$\beta = sideslip\ angle \qquad p = roll\ rate$$
$$r = yaw\ rate \qquad \phi = bank\ angle$$

and the control input vector is defined as

$$u \triangleq \begin{bmatrix} u_{lon}^T & u_{lat}^T \end{bmatrix}^T = \begin{bmatrix} \delta_{elev} & \delta_{thrust} & \delta_{ail} & \delta_{rud} \end{bmatrix}^T. \quad (7)$$

In (7), $\delta_{elev}(t) \in \mathbb{R}$ denotes the elevator deflection angle, $\delta_{thrust}(t) \in \mathbb{R}$ is the control thrust, $\delta_{ail}(t) \in \mathbb{R}$ is the aileron deflection angle, and $\delta_{rud}(t) \in \mathbb{R}$ is the rudder deflection angle.

The disturbance $f(x,t)$ introduced in (1) can represent several bounded nonlinearities. The more promising example of disturbances that can be represented by $f(x,t)$ is the nonlinear form of a selectively extracted portion of the state space matrix $A_{lon} \in \mathbb{R}^{4\times 4}$ that would normally be linearized. This nonlinearity would then be added to the new state space plant by superposition, resulting in the following quasi-linear plant model:

$$\dot{x}_{lon} = A_{lon}^{'} x_{lon} + B_{lon} u_{lon} + f(x_{lon}, t), \quad (8)$$

where $A_{lon}^{'} \in \mathbb{R}^{4\times 4}$ is the state space matrix A_{lon} with the linearized portion removed, and $f(x_{lon}, t) \in \mathbb{R}^4$ denotes the nonlinear disturbances present in the longitudinal dynamics. Some physical examples of $f(x_{lon}, t)$ would be the selective nonlinearities that cannot be ignored, such as when dealing with supermaneuvering vehicles, where post-stall angles of attack and inertia coupling, for example, are encountered. Given that the Osprey is a very benign maneuvering vehicle, $f(x,t)$ in this paper will represent less rigorous nonlinearities for illustrative purposes. A similar technique can be followed with the lateral direction state space representation, where the nonlinear component of A_{lat} is extracted, and a new quasi-linear model for the lateral dynamics is developed as

$$\dot{x}_{lat} = A_{lat}^{'} x_{lat} + B_{lat} u_{lat} + f(x_{lat}, t), \quad (9)$$

where $A_{lat}^{'} \in \mathbb{R}^{4\times 4}$ is the new lateral state matrix with the linearized components removed, and $f(x_{lat}, t) \in \mathbb{R}^4$ denotes the nonlinear disturbances present in the lateral dynamics. Another example of bounded nonlinear disturbances, which can be represented by $f(x,t)$ in (1), is a discrete vertical gust. The formula given in [19], for example, defines such a bounded nonlinearity in the longitudinal axis as

$$f(x_{lon}, t) = \begin{bmatrix} -11.1 \\ 7.2 \\ 37.4 \\ 0 \end{bmatrix} \frac{1}{V_0} \left\{ \frac{U_{ds}}{2} \left[1 - \cos\left(\frac{\pi s}{H} \right) \right] \right\}, \quad (10)$$

where H denotes the distance (between 35 feet and 350 feet) along the airplane's flight path for the gust to reach its peak velocity, V_0 is the forward velocity of the aircraft when it enters the gust, $s \in [0, 2H]$ represents the distance penetrated into the gust (e.g., $s = \int_{t_1}^{t_2} V(t)\, dt$), and U_{ds} is the design gust velocity as specified in [19]. This regulation is intended

to be used to evaluate both vertical and lateral gust loads, so a similar representation can be developed for the lateral dynamics. Another source of bounded nonlinear disturbances that could be represented by $f(x,t)$ is network delay from communication with a ground station.

III. Control Development

To facilitate the subsequent control design, a reference model can be developed as:

$$\dot{x}_m = A_m x_m + B_m \delta \tag{11}$$
$$y_m = C x_m, \tag{12}$$

with $A_m \in \mathbb{R}^{n\times n}$ and $B_m \in \mathbb{R}^{n\times m}$ designed as

$$A_m = \begin{bmatrix} A_{lonm} & 0_{4\times 4} \\ 0_{4\times 4} & A_{latm} \end{bmatrix} \qquad B_m = \begin{bmatrix} B_{lonm} & 0_{4\times 2} \\ 0_{4\times 2} & B_{latm} \end{bmatrix}, \tag{13}$$

where A_m is Hurwitz, $\delta(t) \in \mathbb{R}^m$ is the reference input, $x_m \triangleq \begin{bmatrix} x_{lonm}^T & x_{latm}^T \end{bmatrix}^T \in \mathbb{R}^n$ represents the reference states, $y_m \in \mathbb{R}^m$ are the reference outputs, and C was defined in (2). The lateral and longitudinal reference models were chosen with the specific purpose of decoupling the longitudinal mode velocity and pitch rate as well as decoupling the lateral mode roll rate and yaw rate. In addition to this criterion, the design is intended to exhibit favorable transient response characteristics and to achieve zero steady-state error. Simultaneous and uncorrelated commands are input into each of the longitudinal and lateral model simulations to illustrate that each model indeed behaves as two completely decoupled second order systems.

The contribution in this control design is a robust technique to yield asymptotic tracking for an aircraft in the presence of parametric uncertainty in a non-square input authority matrix and an unknown nonlinear disturbance. To this end, the control law is developed based on the output dynamics, which enables us to transform the uncertain input matrix into a square matrix. By utilizing a feedforward (best guess) estimate of the input uncertainty in the control law in conjunction with a robust control term, we are able to compensate for the input uncertainty. Specifically, based on the assumption that an estimate of the uncertain input matrix can be selected such that a diagonal dominance property is satisfied in the closed-loop error system, asymptotic tracking is proven.[2]

A. Error System

The control objective is to ensure that the system outputs track desired time-varying reference outputs despite unknown, nonlinear, non-LP disturbances in the dynamic model. To quantify this objective, a tracking error, denoted by $e(t) \in \mathbb{R}^m$, is defined as

$$e = y - y_m = C(x - x_m). \tag{14}$$

[2]Preliminary simulation results show that this assumption is mild in the sense that a wide range of estimates satisfy this requirement.

To facilitate the subsequent analysis, a filtered tracking error [20], denoted by $r(t) \in \mathbb{R}^m$, is defined as:

$$r \triangleq \dot{e} + \alpha e, \tag{15}$$

where $\alpha \in \mathbb{R}^{m\times m}$ denotes a matrix of positive, constant control gains.

Remark 1: It can be shown that the system in (1) and (2) is bounded input bounded output (BIBO) stable in the sense that the unmeasurable states $x_u \in \mathbb{R}^{n-m}$ and the corresponding time derivatives are bounded as

$$\|x_u\| \le c_1 \|z\| + \zeta_{xu} \qquad \|\dot{x}_u\| \le c_2 \|z\| + \zeta_{\dot{x}u}, \tag{16}$$

where $z \in \mathbb{R}^{2m}$ is defined as

$$z \triangleq \begin{bmatrix} e^T & r^T \end{bmatrix}^T, \tag{17}$$

and $c_1, c_2, \zeta_{xu}, \zeta_{\dot{x}u} \in \mathbb{R}$ are known positive bounding constants, provided the control input $u(t)$ remains bounded during close-loop operation.

The open-loop tracking error dynamics can be developed by taking the time derivative of (15) and utilizing the expressions in (1), (2), (11), and (12) to obtain the following expression:

$$\dot{r} = \tilde{N} + N_d + \Omega(\dot{u} + \alpha u) - e, \tag{18}$$

where the auxiliary function $\tilde{N}(x, \dot{x}, e, \dot{e}) \in \mathbb{R}^m$ is defined as

$$\tilde{N} \triangleq CA(\underline{\dot{x}} - \underline{\dot{x}}_m) + \alpha CA(\underline{x} - \underline{x}_m) + CA(\dot{x}_{\rho u} + \alpha x_{\rho u}) + e, \tag{19}$$

the auxiliary function $N_d\left(x_m, \dot{x}_m, \delta, \dot{\delta}\right)$ is defined as

$$\begin{aligned} N_d = {} & CA(\underline{\dot{x}}_m + \alpha \underline{x}_m) + C\left(\dot{f}(x,t) + \alpha f(x,t)\right) \\ & - CA_m(\dot{x}_m + \alpha x_m) - CB_m\left(\dot{\delta} + \alpha\delta\right) \\ & + CA(\dot{x}_{\zeta u} + \alpha x_{\zeta u}), \end{aligned} \tag{20}$$

and the constant, unknown matrix $\Omega \in \mathbb{R}^{m\times m}$ is defined as

$$\Omega \triangleq CB. \tag{21}$$

In (19) and (20), $x_{\rho u}(t), \dot{x}_{\rho u}(t) \in \mathbb{R}^n$ contain the portions of $x_u(t)$ and $\dot{x}_u(t)$, respectively, that can be upper bounded by functions of the states, $x_{\zeta u}(t), \dot{x}_{\zeta u}(t) \in \mathbb{R}^n$ contain the portions of $x_u(t)$ and $\dot{x}_u(t)$ that can be upper bounded by known constants (i.e., see (16)), $\underline{x}(t) \in \mathbb{R}^n$ contains the measurable states (i.e., $x(t) = \underline{x}(t) + x_{\rho u}(t) + x_{\zeta u}(t)$), and $\underline{x}_m(t) \in \mathbb{R}^n$ contains the reference states corresponding to the measurable states $\underline{x}(t)$. The quantities $\tilde{N}(x, \dot{x}, e, \dot{e})$ and $N_d\left(x_m, \dot{x}_m, \delta, \dot{\delta}\right)$ and the derivative $\dot{N}_d\left(x_m, \dot{x}_m, \ddot{x}_m, \delta, \dot{\delta}, \ddot{\delta}\right)$ can be upper bounded as follows:

$$\left\|\tilde{N}\right\| \le \rho(\|z\|)\|z\| \qquad \|N_d\| \le \zeta_{N_d} \qquad \left\|\dot{N}_d\right\| \le \zeta_{\dot{N}_d}, \tag{22}$$

where $\zeta_{N_d}, \zeta_{\dot{N}_d} \in \mathbb{R}$ are known positive bounding constants, and the function $\rho(\|z\|)$ is a positive, globally invertible, nondecreasing function. Based on the expression in (18) and

the subsequent stability analysis, the control input is designed as

$$u = -\alpha \int_0^t u(\tau)\, d\tau - (k_s+1)\hat{\Omega}^{-1} e(t) + (k_s+1)\hat{\Omega}^{-1} e(0) - \int_0^t k_\gamma \hat{\Omega}^{-1} sgn(r(\tau))\, d\tau - \hat{\Omega}^{-1} \int_0^t [(k_s+1)\alpha e(\tau) + \beta sgn(e(\tau))]\, d\tau, \quad (23)$$

where $\beta, k_s, k_\gamma \in \mathbb{R}^{m\times m}$ are diagonal matrices of positive, constant control gains, α was defined in (15), and the constant feedforward estimate $\hat{\Omega} \in \mathbb{R}^{m\times m}$ is defined as

$$\hat{\Omega} \triangleq CB. \quad (24)$$

To simplify the notation in the subsequent stability analysis, the constant auxiliary matrix $\tilde{\Omega} \in \mathbb{R}^{m\times m}$ is defined as

$$\tilde{\Omega} \triangleq \Omega \hat{\Omega}^{-1}, \quad (25)$$

where $\tilde{\Omega}$ can be separated into diagonal and off-diagonal components as

$$\tilde{\Omega} = \Lambda + \Delta, \quad (26)$$

where $\Lambda \in \mathbb{R}^{m\times m}$ contains only the diagonal elements of $\tilde{\Omega}$, and $\Delta \in \mathbb{R}^{m\times m}$ contains the off-diagonal elements.

After substituting the time derivative of (23) into (18), the following closed-loop error system is obtained:

$$\dot{r} = \tilde{N} + N_d - (k_s+1)\tilde{\Omega} r - k_\gamma \tilde{\Omega} sgn(r) - \tilde{\Omega}\beta sgn(e(t)) - e. \quad (27)$$

Assumption 3: The constant estimate $\hat{\Omega}$ given in (24) is selected such that the following condition is satisfied:

$$\lambda_{\min}(\Lambda) - \|\Delta\| > \varepsilon, \quad (28)$$

where $\varepsilon \in \mathbb{R}$ is a known positive constant, and $\lambda_{\min}(\cdot)$ denotes the minimum eignenvalue of the argument. Preliminary testing results show this assumption is mild in the sense that (28) is satisfied for a wide range of $\hat{\Omega} \neq \Omega$.

Remark 2: A possible deficit of this control design is that the acceleration-dependent term $r(t)$ appears in the control input given in (23). This is undesirable from a controls standpoint; however, many aircraft controllers are designed based on the assumption that acceleration measurements are available [21]–[25]. Further, from (23), the sign of the acceleration is all that is required for measurement in this control design.

IV. Stability Analysis

Theorem 1: The controller given in (23) ensures that the output tracking error is regulated in the sense that

$$\|e(t)\| \to 0 \qquad \text{as } t \to \infty, \quad (29)$$

provided the control gain k_s introduced in (23) is selected sufficiently large (see the subsequent stability proof), and β and k_γ are selected according to the following sufficient conditions:

$$\beta > \frac{\left(\zeta_{N_d} + \frac{1}{\alpha}\zeta_{\dot{N}_d}\right)}{\lambda_{\min}(\Lambda)} \qquad k_\gamma > \frac{\sqrt{m}\beta\|\Delta\|}{\varepsilon}, \quad (30)$$

where ζ_{N_d} and $\zeta_{\dot{N}_d}$ were introduced in (22), ε was defined in (28), and Λ and Δ were introduced in (26).

The following lemma is utilized in the proof of Theorem 1.

Lemma 1: Let $\mathcal{D} \subset \mathbb{R}^{2m+1}$ be a domain containing $w(t) = 0$, where $w(t) \in \mathbb{R}^{2m+1}$ is defined as

$$w(t) \triangleq \begin{bmatrix} z^T & \sqrt{P(t)} \end{bmatrix}^T, \quad (31)$$

and the auxiliary function $P(t) \in \mathbb{R}$ is defined as

$$P(t) \triangleq \beta\|e(0)\|\|\Lambda\| - e(0)^T N_d(0) + \sqrt{m}\int_0^t \beta\|\Delta\|\|r(\tau)\|\, d\tau - \int_0^t L(\tau)\, d\tau. \quad (32)$$

The auxiliary function $L(t) \in \mathbb{R}$ in (32) is defined as

$$L(t) \triangleq r^T\left(N_d(t) - \beta\tilde{\Omega} sgn(e)\right). \quad (33)$$

Provided the sufficient conditions in (30) is satisfied, the following inequality can be obtained:

$$\int_0^t L(\tau)\, d\tau \leq \beta\|e(0)\|\|\Lambda\| - e(0)^T N_d(0) + \sqrt{m}\int_0^t \beta\|\Delta\|\|r(\tau)\|\, d\tau. \quad (34)$$

Hence, (34) can be used to conclude that $P(t) \geq 0$.

Proof: (See Theorem 1) Let $V(w,t) : \mathcal{D}\times[0,\infty) \to \mathbb{R}$ be a continuously differentiable, positive definite function defined as

$$V \triangleq \frac{1}{2}e^T e + \frac{1}{2}r^T r + P, \quad (35)$$

where $e(t)$ and $r(t)$ are defined in (14) and (15), respectively, and the positive definite function $P(t)$ is defined in (32). The positive definite function $V(w,t)$ satisfies the inequality

$$U_1(w) \leq V(w,t) \leq U_2(w), \quad (36)$$

provided the sufficient condition introduced in (30) is satisfied. In (36), the continuous, positive definite functions $U_1(w), U_2(w) \in \mathbb{R}$ are defined as

$$U_1 \triangleq \frac{1}{2}\|w\|^2 \qquad U_2 \triangleq \|w\|^2. \quad (37)$$

After taking the derivative of (35) and utilizing (15), (26), (27), (32), and (33), $\dot{V}(w,t)$ can be expressed as

$$\dot{V}(w,t) = -\alpha e^T e + r^T\tilde{N} - (k_s+1)r^T\Lambda r - (k_s+1)r^T\Delta r + \sqrt{m}\beta\|r\|\|\Delta\| - k_\gamma r^T\Delta sgn(r) - k_\gamma r^T\Lambda sgn(r). \quad (38)$$

By utilizing (22), $\dot{V}(w,t)$ can be upper bounded as

$$\dot{V}(w,t) \leq -\alpha e^T e - \varepsilon\|r\|^2 - k_s\varepsilon\|r\|^2 + \rho(\|z\|)\|r\|\|z\| + \left[-k_\gamma\varepsilon + \sqrt{m}\beta\|\Delta\|\right]\|r\|. \quad (39)$$

Clearly, if the second of equations (30) is satisfied, the bracketed term in (39) is negative, and $\dot{V}(w,t)$ can be upper

bounded using the squares of the components of $z(t)$ as follows:

$$\dot{V}(w,t) \leq -\alpha \|e\|^2 - \varepsilon \|r\|^2 + \left[\rho(\|z\|)\|r\|\|z\| - k_s \varepsilon \|r\|^2\right]. \quad (40)$$

Completing the squares for the bracketed terms in (40) yields

$$\dot{V}(w,t) \leq -\eta_3 \|z\|^2 + \frac{\rho^2(\|z\|)\|z\|^2}{4k_s\varepsilon}, \quad (41)$$

where $\eta_3 \triangleq \min\{\alpha, \varepsilon\}$, and $\rho(\|z\|)$ is introduced in (22). The following expression can be obtained from (41):

$$\dot{V}(w,t) \leq -U(w), \quad (42)$$

where $U(w) = c\|z\|^2$, for some positive constant $c \in \mathbb{R}$, is a continuous, positive semi-definite function that is defined on the following domain:

$$\mathcal{D} \triangleq \left\{ w \in \mathbb{R}^{2m+1} \mid \|w\| < \rho^{-1}\left(2\sqrt{\eta_3 k_s \varepsilon}\right)\right\}. \quad (43)$$

The inequalities in (36) and (42) can be used to show that $V(t) \in \mathcal{L}_\infty$ in $\mathcal{D}$; hence $e(t), r(t) \in \mathcal{L}_\infty$ in $\mathcal{D}$. Given that $e(t), r(t) \in \mathcal{L}_\infty$ in $\mathcal{D}$, standard linear analysis methods can be used to prove that $\dot{e}(t) \in \mathcal{L}_\infty$ in $\mathcal{D}$ from (15). Since $e(t), \dot{e}(t) \in \mathcal{L}_\infty$ in $\mathcal{D}$, the assumption that $y_m, \dot{y}_m \in \mathcal{L}_\infty$ in $\mathcal{D}$ can be used along with (14) to prove that $y, \dot{y} \in \mathcal{L}_\infty$ in $\mathcal{D}$. Given that $r(t) \in \mathcal{L}_\infty$ in $\mathcal{D}$, the assumption that $\hat{\Omega}^{-1} \in \mathcal{L}_\infty$ in $\mathcal{D}$ can be used along with the time derivative of (23) to show that $\dot{u}(t) \in \mathcal{L}_\infty$ in $\mathcal{D}$. Further, Equation 2.78 of [26] can be used to show that $\dot{u}(t)$ can be upper bounded as $\dot{u}(t) \leq -\alpha u(\tau) + M$, $\forall t \geq 0$, where $M \in \mathbb{R}^+$ is a bounding constant. Theorem 1.1 of [27] can then be utilized to show that $u(t) \in \mathcal{L}_\infty$ in $\mathcal{D}$. Hence, (27) can be used to show that $\dot{r}(t) \in \mathcal{L}_\infty$ in $\mathcal{D}$. Since $\dot{e}(t), \dot{r}(t) \in \mathcal{L}_\infty$ in $\mathcal{D}$, the definitions for $U(w)$ and $z(t)$ can be used to prove that $U(w)$ is uniformly continuous in $\mathcal{D}$.

Let $S \subset \mathcal{D}$ denote a set defined as follows:

$$S \triangleq \left\{ w(t) \subset \mathcal{D} \mid U_2(w(t)) < \frac{1}{2}\left(\rho^{-1}\left(2\sqrt{\varepsilon \eta_3 k_s}\right)\right)^2\right\}. \quad (44)$$

Theorem 8.4 of [28] can now be invoked to state that

$$c\|z\|^2 \to 0 \quad as \quad t \to \infty \quad \forall w(0) \in S. \quad (45)$$

Based on the definition of z, (45) can be used to show that

$$\|e(t)\| \to 0 \quad as \quad t \to \infty \quad \forall w(0) \in S. \quad (46)$$

■

V. Simulation Results

A numerical simulation was created to test the efficacy of the proposed controller. The simulation is based on the aircraft state space system given in (1) and (2), where the numerical values for the state matrix A and input authority matrix B (e.g., see (3)-(7)) are based on the linearized model for the Osprey aircraft.[3] The reference model for the simulation is represented by the state space system given in (11)-(13), where A_{lonm} and A_{latm} are Hurwitz.[4]

The nonlinear disturbance terms $f(x_{lon}, t)$ and $f(x_{lat}, t)$ introduced in (8) and (9), respectively, are defined as

$$f(x_{lon}, t) = \begin{bmatrix} -9.81\sin\theta + g(x) & 0 & 0 & 0 \end{bmatrix}^T \quad (47)$$

$$f(x_{lat}, t) = \begin{bmatrix} 0.39\sin\phi & 0 & 0 & 0 \end{bmatrix}^T, \quad (48)$$

where $g(x)$ represents a disturbance due to a discrete vertical wind gust as defined in (10), where $U_{ds} = 10.12\ m/s$, $H = 15.24\ m$, and $V_0 = 25\ m/s$ (cruise velocity). The remainder of the additive disturbances in (47) and (48) represent nonlinearities not captured in the linearized state space model (e.g., due to small angle assumptions). All states and control inputs were initialized to zero for the simulation.

Remark 3: For the estimate $\hat{B}_{lon}$ used in the simulation, the inequality in (28) is satisfied. Specifically, the choice for $\hat{B}_{lon}$ yields

$$\lambda_{\min}(\Lambda) = 0.6450 > 0.0046 = \|\Delta\|. \quad (49)$$

In order to develop a realistic stepping stone to an actual experimental demonstration of the proposed aircraft controller, the simulation parameters were selected based on detailed data analyses and specifications. The sensor noise values are based upon Cloud Cap Technology's Piccolo Autopilot and analysis of data logged during straight and level flight. The thrust limit and estimated rate limit was measured via a static test using a fish scale. The control surface rate and position limits were determined via the geometry of the control surface linkages in conjunction with the detailed specifications sheet given with the Futaba S3010 standard ball bearing servo.

The objectives for the longitudinal controller simulation are to track pitch rate and forward velocity commands. Figs. 2-3 show the simulation results of the closed-loop longitudinal system with control gains selected as follows (e.g., see (21) and (23))[5]:

$$\beta = diag\{\ 0.1 \quad 130\ \} \qquad k_s = diag\{\ 0.2 \quad 160\ \}$$
$$\alpha = diag\{\ 0.7 \quad 0.1\ \} \qquad k_\gamma = 0.1 I_{2\times 2},$$

where the notation $I_{j\times j}$ denotes the $j \times j$ identity matrix. Fig. 2 shows the reference and actual pitch rates during closed-loop operation, and Fig. 3 shows the reference and actual forward velocity responses.

VI. Conclusion

An aircraft controller is presented, which achieves asymptotic tracking control of a model reference system where the plant dynamics contain input uncertainty and a bounded non-LP disturbance. The developed controller exhibits the desirable characteristic of tracking the specified decoupled reference model. To achieve the result, a novel robust control

[3]The numerical values for the Osprey aircraft are only used in the simulation to generate the uncertain plant model for the aircraft, the values are not used in the control design.

[4]Although both the longitudinal and lateral subsystems were simulated, only the longitudinal simulation results are presented in this section for the sake of brevity.

[5]The k_γ used in the longitudinal controller simulation does not satisfy the sufficient condition given in (30); however, this condition is not necessary for stability, it is sufficient for the Lyapunov stability proof.

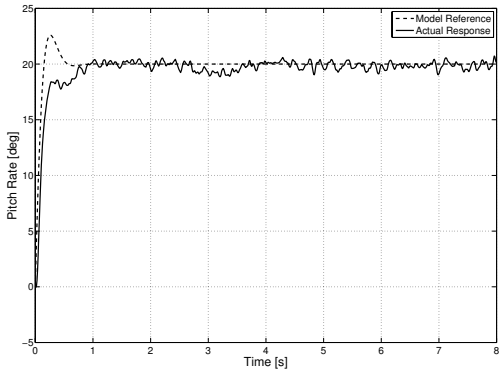

Fig. 2. Pitch rate response during closed-loop longitudinal controller operation.

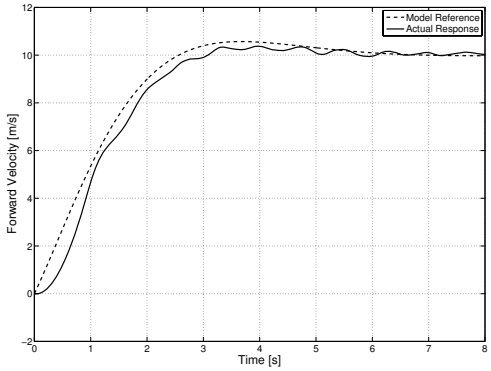

Fig. 3. Forward velocity response during closed-loop longitudinal controller operation.

technique is combined with a RISE control structure. A Lyapunov-based stability analysis is provided to verify the theoretical result, and simulation results demonstrate the robustness of the controller to sensor noise, exogenous perturbations, parametric uncertainty, and plant nonlinearities, while simultaneously exhibiting the capability to emulate a reference model designed offline.

REFERENCES

[1] A. Moutinho and J. R. Azinheira, "Stability and robustness analysis of the AURORA airship control system using dynamic inversion," in *Proc. of Int'l Conf. on Robotics and Automation*, Barcelona, Spain, April 2005, pp. 2265–2270.

[2] M. W. Oppenheimer and D. B. Doman, "Control of an unstable, nonminimum phase hypersonic vehicle model," in *Proc. of the IEEE Aerospace Conf.*, Big Sky, MT, Mar. 2006, pp. 1–7.

[3] S. Onori, P. Dorato, S. Galeani, and C. Abdallah, "Finite time stability design via feedback linearization," in *Proc. of Conf. on Decision and Control, and the European Control Conf.*, Seville, Spain, Dec. 2005, pp. 4915–4920.

[4] Z. Szabo, P. Gaspar, and J. Bokor, "Tracking design for Wiener systems based on dynamic inversion," in *Proc. of Int'l Conf. on Control Applications*, Munich, Germany, Oct. 2006, pp. 1386–1391.

[5] J. Chen, D. Li, X. Jiang, and X. Sun, "Adaptive feedback linearization control of a flexible spacecraft," in *Proc. of Conf. on Intelligent Systems Design and Applications*, Jinan, China, Oct. 2006, pp. 225–230.

[6] A. D. Ngo and D. B. Doman, "Dynamic inversion-based adaptive/reconfigurable control of the X-33 on ascent," in *Proc. of IEEE Aerospace Conference*, Big Sky, MT, Mar. 2006, pp. 2683–2697.

[7] M. D. Tandale and J. Valasek, "Adaptive dynamic inversion control of a linear scalar plant with constrained control inputs," in *Proc. of American Control Conf.*, Portland, OR, June 2005, pp. 2064–2069.

[8] N. Hovakimyan, E. Lavretsky, and A. Sasane, "Dynamic inversion for nonaffine-in-control systems via time-scale separation: Part I," in *Proc. of American Control Conf.*, Portland, OR, June 2005, pp. 3542–3547.

[9] E. Lavretsky and N. Hovakimyan, "Adaptive dynamic inversion for nonaffine-in-control systems via time-scale separation: part II," in *Proc. of American Control Conf.*, Portland, OR, June 2005, pp. 3548–3553.

[10] X.-. J. Liu, F. Lara-Rosano, and C. W. Chan, "Model-reference adaptive control based on neurofuzzy networks," *IEEE Trans. Syst., Man, Cybern. C*, vol. 34, no. 3, pp. 302–309, Aug. 2004.

[11] A. Calise and R. Rysdyk, "Nonlinear adaptive flight control using neural networks," *IEEE Control System Magazine*, vol. 18, no. 6, pp. 14–25, Dec. 1998.

[12] J. Leitner, A. Calise, and J. V. R. Prasad, "Analysis of adaptive neural networks for helicopter flight controls," *J. Guidance, Control and Dynamics*, vol. 20, no. 5, pp. 972–979, Sept. 1997.

[13] Y. Shin, "Neural network based adaptive control for nonlinear dynamic regimes," Ph.D. dissertation, Georgia Technical Institute, November 2005.

[14] E. Lavretsky and N. Hovakimyan, "Adaptive compensation of control dependent modeling uncertainties using time-scale separation," in *Proc. of Conf. on Decision and Control, and the European Control Conf.*, Seville, Spain, Dec. 2005, pp. 2230–2235.

[15] B. Xian, D. M. Dawson, M. S. de Queiroz, and J. Chen, "A continuous asymptotic tracking control strategy for uncertain nonlinear systems," *IEEE Transactions on Automatic Control*, vol. 49, no. 7, pp. 1206–1211, July 2004.

[16] P. M. Patre, W. MacKunis, C. Makkar, and W. E. Dixon, "Asymptotic tracking for systems with structured and unstructured uncertainties," in *Proc. of Conf. on Decision and Control*, San Diego, CA, Dec. 2006, pp. 441–446.

[17] B. Xian, M. S. de Queiroz, and D. M. Dawson, *A Continuous Control Mechanism for Uncertain Nonlinear Systems in Optimal Control, Stabilization, and Nonsmooth Analysis*. Heidelberg, Germany: Springer-Verlag, 2004.

[18] A. Behal, D. M. Dawson, W. E. Dixon, and Y. Fang, "Tracking and regulation control of an underactuated surface vessel with nonintegrable dynamics," in *Proc. of Conf. on Decision and Control*, vol. 3, Sydney, Australia, Dec. 2000, pp. 2150–2155.

[19] Department of Transportation, "Airworthiness Standards: Transport category airplanes," in *Federal Aviation Regulations - Part 25*, Washington, DC, 1996.

[20] F. L. Lewis, C. T. Abdallah, and D. M. Dawson, *Control of Robot Manipulators*. New York, NY: MacMillan, 1993.

[21] B. S. Davis, T. Denison, and J. Kaung, "A monolithic high-g SOI-MEMS accelerometer for measuring projectile launch and flight accelerations," in *Proc. of Conf. on Sensors*, Vienna, Austria, Oct. 2004, pp. 296–299.

[22] V. Janardhan, D. Schmitz, and S. N. Balakrishnan, "Development and implementation of new nonlinear control concepts for a UA," in *Proc. of Digital Avionics Systems Conf.*, Salt Lake City, UT, Oct. 2004, pp. 12.E.5–121–10.

[23] T. Wagner and J. Valasek, "Digital autoland control laws using quantitative feedback theory and direct digital design," *J. Guidance, Control and Dynamics*, vol. 30, no. 5, pp. 1399–1413, Sept. 2007.

[24] M. Bodson, "Multivariable adaptive algorithms for reconfigurable flight control," in *Proc. of Conf. on Decision and control*, Lake Buena Vista, FL, Dec. 1994, pp. 12.E.5–121–10.

[25] B. J. Bacon, A. J. Ostroff, and S. M. Joshi, "Reconfigurable NDI controller using inertial sensor failure detection & isolation," *IEEE Trans. Aerosp. Electron. Syst.*, vol. 37, no. 4, pp. 1373–1383, Oct. 2001.

[26] G. Tao, *Adaptive Control Design and Analysis*, S. Haykin, Ed. Wiley-Interscience, 2003.

[27] D. Dawson, M. Bridges, and Z. Qu, *Nonlinear Control of Robotic Systems for Environmental Waste and Restoration*. Englewood Cliffs, New Jersey: Prentice Hall PTR, 1995.

[28] H. K. Khalil, *Nonlinear Systems*, 3rd ed. Upper Saddle River, NJ: Prentice Hall, 2002.